# Реликтовое излучение.

1924г — Гамов и др. (указание).

1965г., Пензиас и Вилсон, $L = 7.4$ см (Bell lab.)

изотропное излучение соот-ее излучению абсолютно чёрного тела

$$T = 3.5 \pm 1.0 \text{ K}. \quad (\text{Wilson}, 1979)$$

В настоящее время $\lambda : (75 \text{ см} \div 8 \text{ мм})$ — ОК.

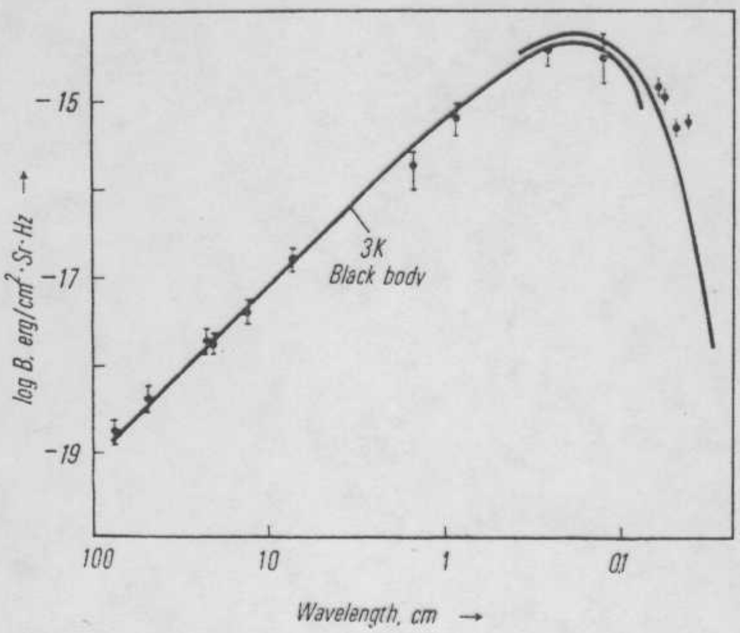


$$T_{ри} = 2.728 \pm 0.002 \quad \text{K} \quad (\text{COBE}) \;!!!$$

$$N_\gamma^{ри} = 412 \ \frac{1}{\text{см}^3}$$

Выделенная система отсчёта, связанная с РИ.

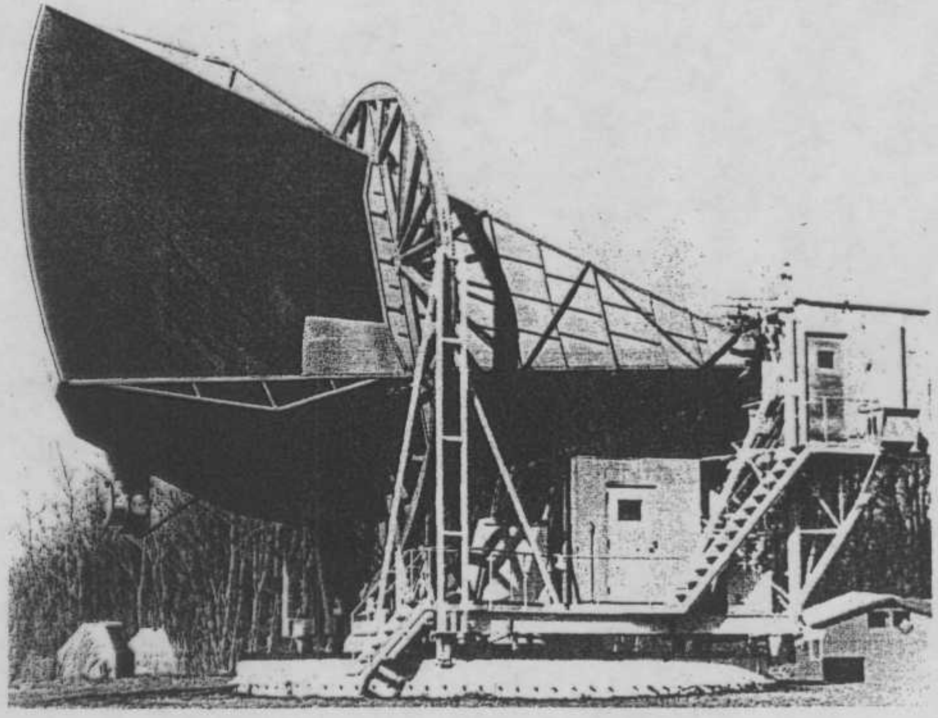

$$T_{\text{ант.}}^{\text{расч.}} = 18.9\ \text{K}$$

$$T_{\text{ант.}}^{\text{изм}} = 22.2 \pm 1\ \text{K}.$$

$T_B^{\gamma} = 2.7$ K

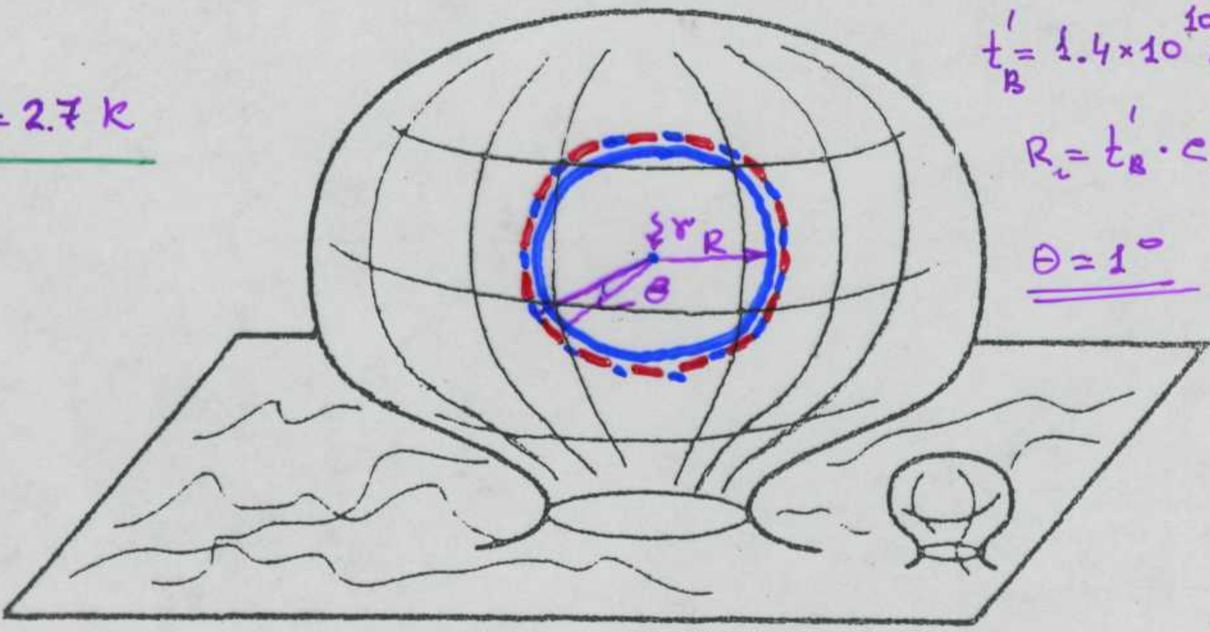


$t'_B = 1.4 \times 10^{10}$ лет

$R_r = t'_B \cdot c \gg r_r$

$\theta = 1^{\circ}$

$T_B^{\gamma} \simeq 3000$ K

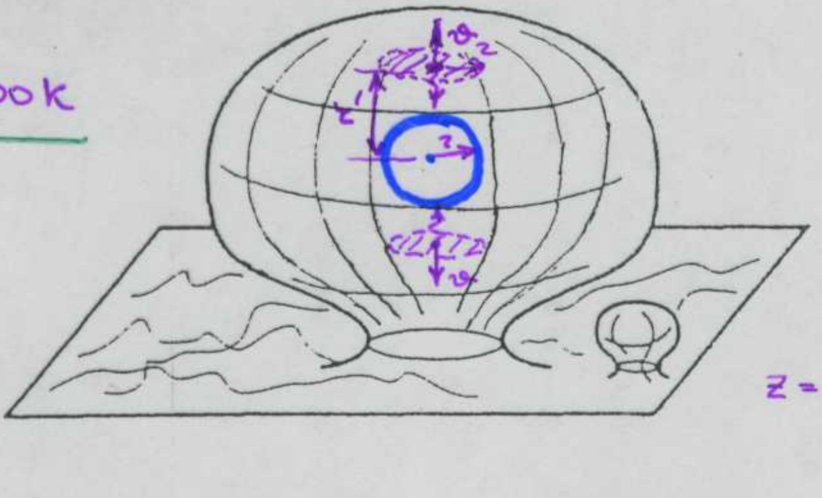


$t_B = 300.000$ лет

$r_r = t_B \cdot c$

$\vartheta = H' \cdot r'$, $(z = 1100)$

$$z = \frac{\Delta\lambda}{\lambda} = \frac{\lambda_{пр} - \lambda_{ист}}{\lambda_{ист}}$$

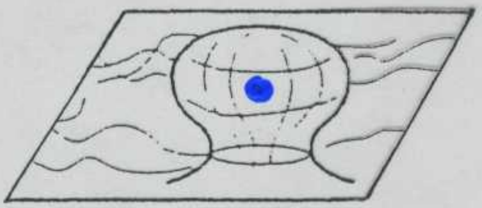

$t_B = 1000$ лет

# Изотропия реликтового излучения.

$T_{рu} = 2.728 \pm 0.002\ K$ (COBE) (1989 ÷ 1993 гг)

$\frac{\Delta T_{рu}}{T_{рu}} < 10^{-5}$ !!!

1) $\lambda = 1 \div 3.5\ \mu m$
2) $\lambda = 100\mu m \div 1\ cm$
3) $f = 31.5,\ 53,\ 90$ ГГц.

$R_{вид.\,Всел.} = c \cdot T_{Всел}$ $(1.4 \times 10^{10}$ лет$)$

$v = H \cdot c \cdot t_{Всел}$, $(Z \simeq 1100)$

$$Z = \frac{\Delta\lambda}{\lambda} = \frac{\lambda_{приём} - \lambda_{изл}}{\lambda_{изл}}$$

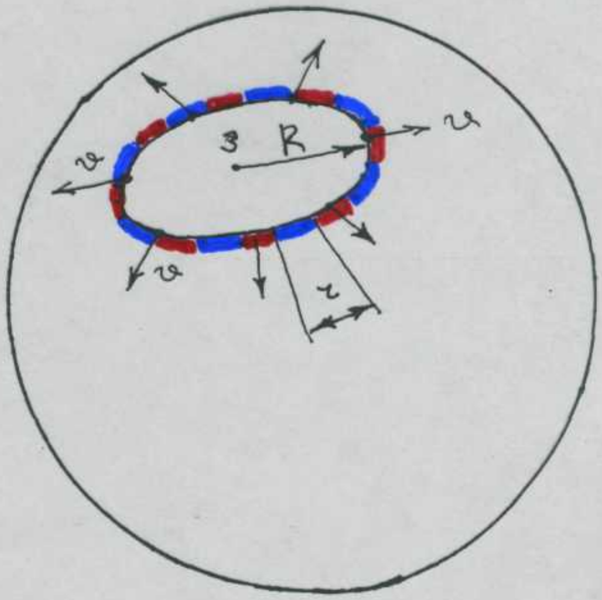


$\Rightarrow T = 3000\ K \rightarrow 2.7\ K$

$\tau = c \cdot t_{Всел}(3000 k)$, $t_{Всел}(3000 k) = 300.000$ лет

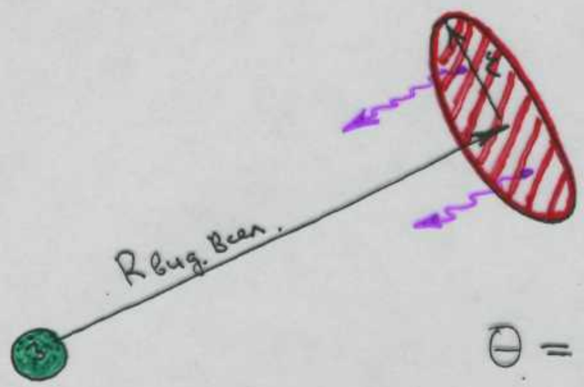


$\Theta = \frac{\tau}{R} \simeq 1^\circ$ (2 ⌀ луны)

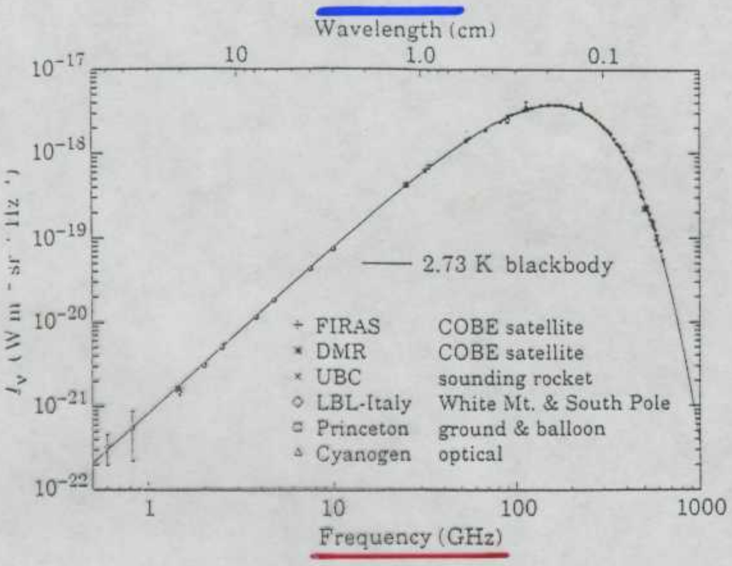


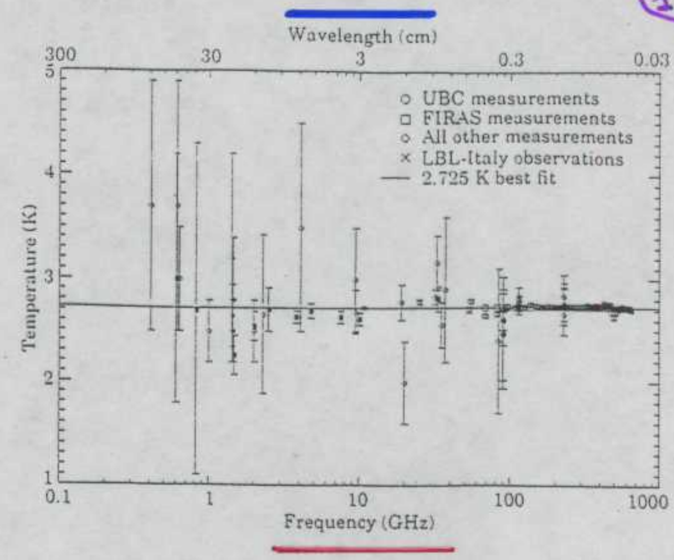


$$\frac{\Delta T_{РИ}}{T_{РИ}} < 10^{-5}$$

после учёта тривиальных анизотропий:

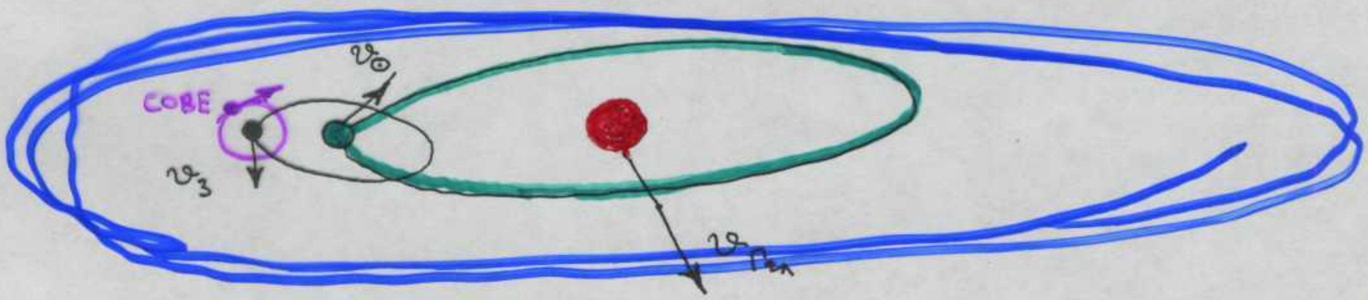


$v_{Гал} = (627 \pm 22)$ км/с
$v_\odot = (371 \pm 0.5)$ км/с
} дипольная анизотропия $\quad \frac{\Delta T}{T} = 1.23 \times 10^{-3}$.

$v_З =$

⋮

Объяснение изотропии РИ → инфляционная модель Вселенно

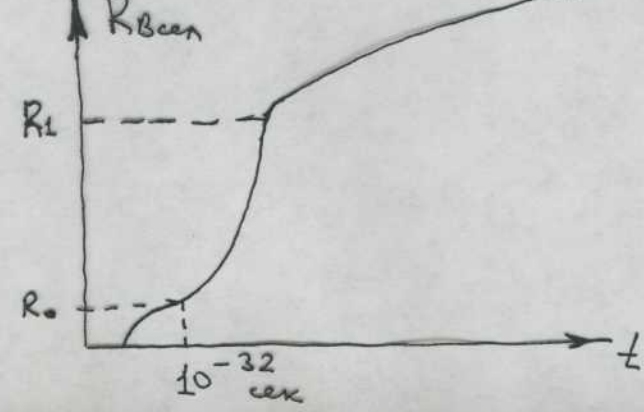


$R_0 \sim 10^{-20}$ см

$\frac{R_1}{R_0} \simeq 10^{3260}$ раз !!!

$\tau \sim 10^{-32}$ сек !!!

# Анизотропия реликтового излучения.

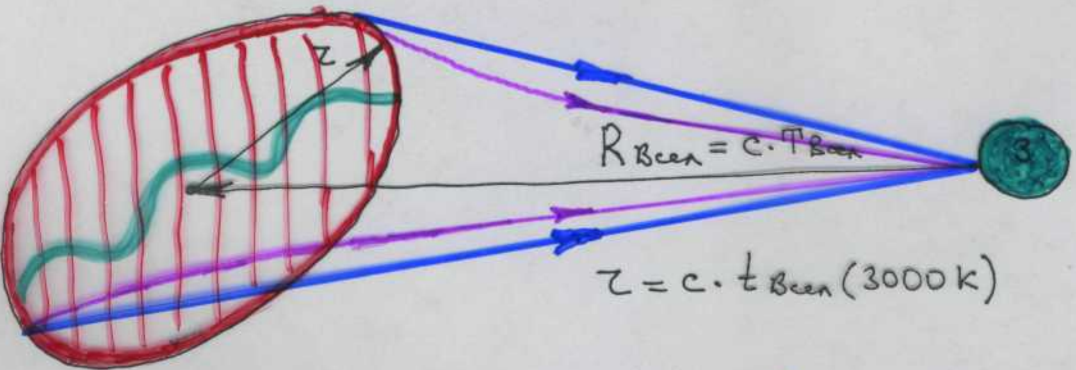


$r = c \cdot t_{всел}\,(3000\,K)$ $\theta < \Theta$ !

$\Rightarrow$ значение $\Omega_{tot} = \Omega_m + \Omega_\Lambda = \dfrac{\rho_{всел}}{\rho_c}$

## Источники анизотропии РИ.

- Звуковые волны в плазме

  $E_{\gamma_1} > E_{\gamma_2}$

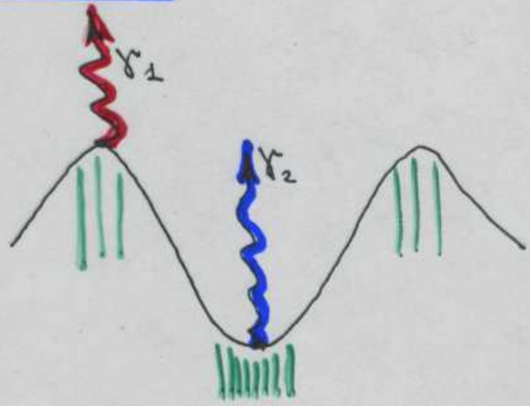


- Гравитационное красное смещение

  $E_{\gamma_1} > E_{\gamma_2}$

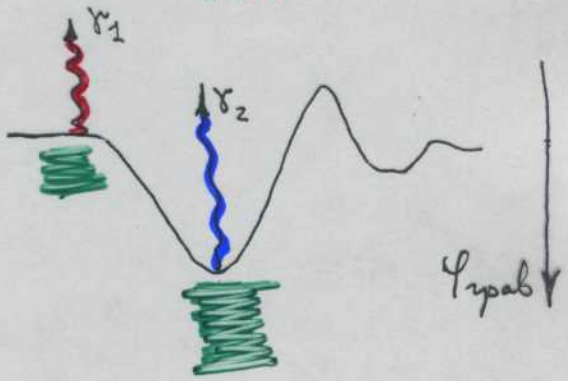


- Доплер эффект

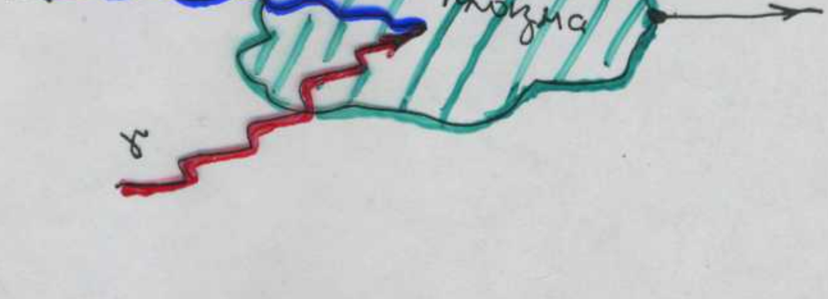


$E_\gamma > E'_\gamma$

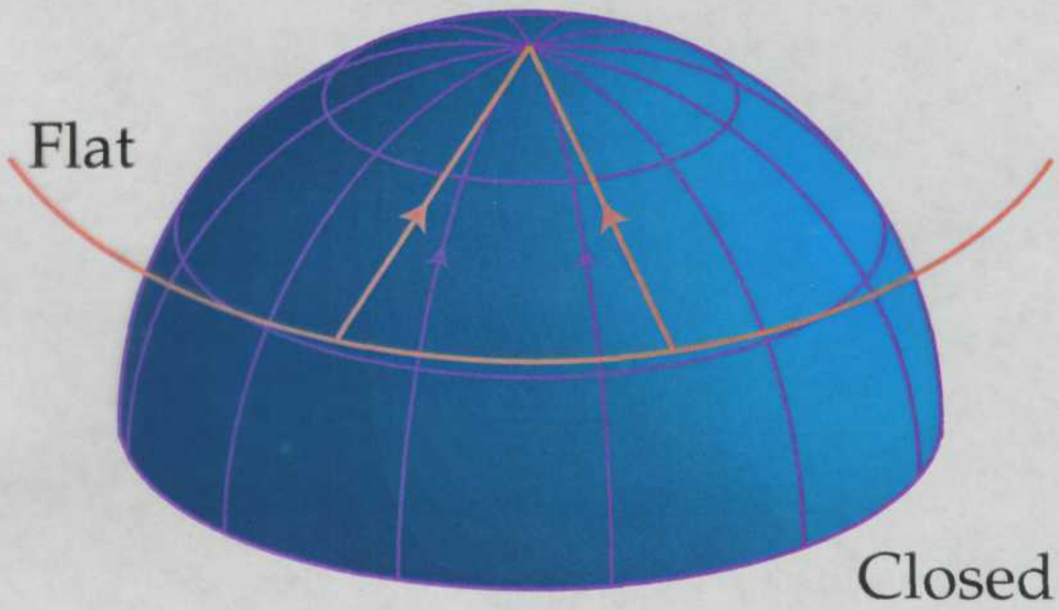
Flat
Closed

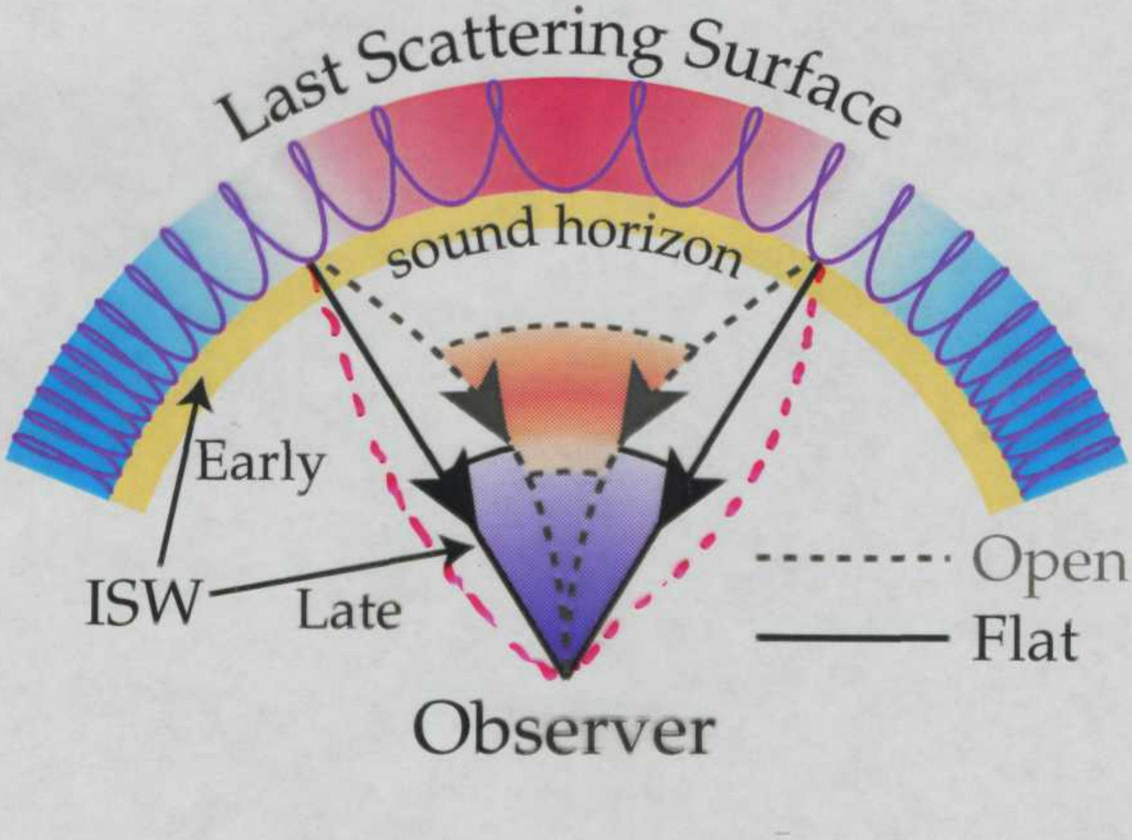
Last Scattering Surface
sound horizon
Early
ISW
Late
Open
Flat
Observer

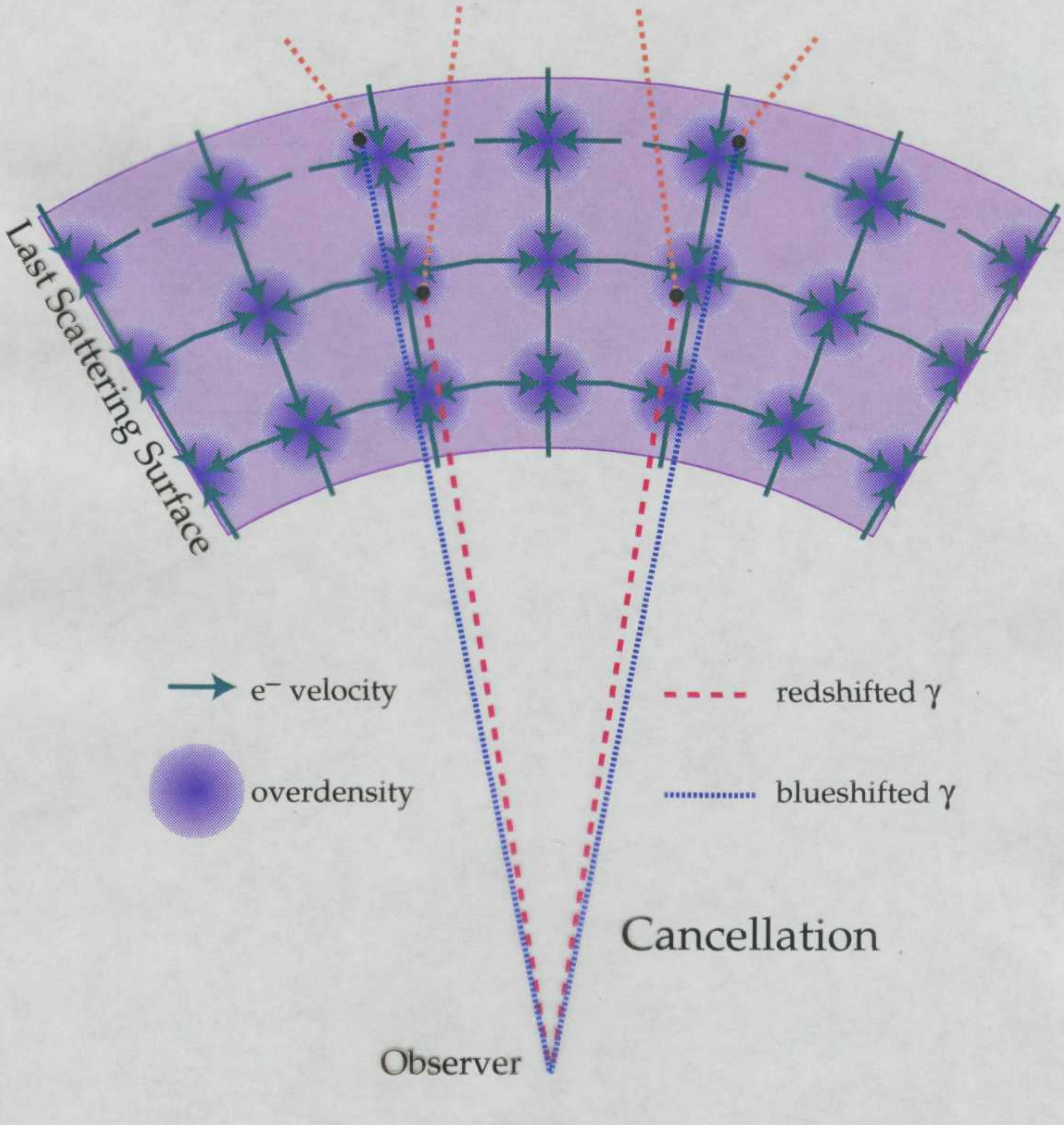
Last Scattering Surface
e⁻ velocity
overdensity
redshifted γ
blueshifted γ
Cancellation
Observer

# Параметризация флуктуаций температуры.

разложение по мультиполям

$$\frac{\Delta T}{T}(\vec{x}) = \sum_{lm}{}' a_{lm}\cdot Y_{lm}(\theta, \varphi)$$

$a_{lm}$ - амплитуда мультиполя.

Спектр флуктуаций определяется из автокорреляционной ф-ии:

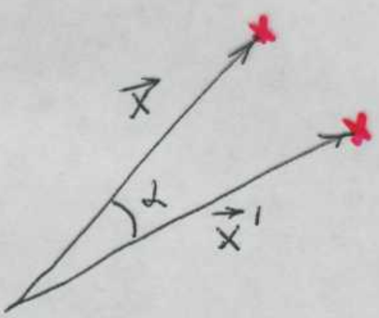


$$C(\alpha) = \left\langle \frac{\Delta T}{T}(\vec{x})\cdot \frac{\Delta T}{T}(\vec{x}')\right\rangle$$

$$= \frac{1}{4\pi}\sum_{l}{}'\left[(2l+1)\,C_l\cdot P_l(\cos\alpha)\right].$$

$\langle\rangle$ усреднение по всему небу,

$(\vec{x}\cdot\vec{x}') = \cos\alpha$.

$C_l$ - мультипольный момент ($C_2$ - квадру-ый)

$C_l$ - опре-ся флук-ми на углах $\theta \sim \frac{\pi}{l}$

$W_l = l(l+1)C_l$ - спектр мощности

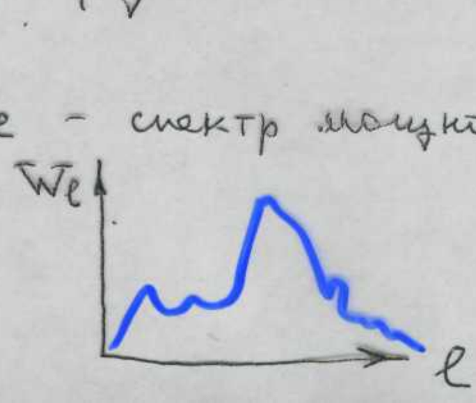

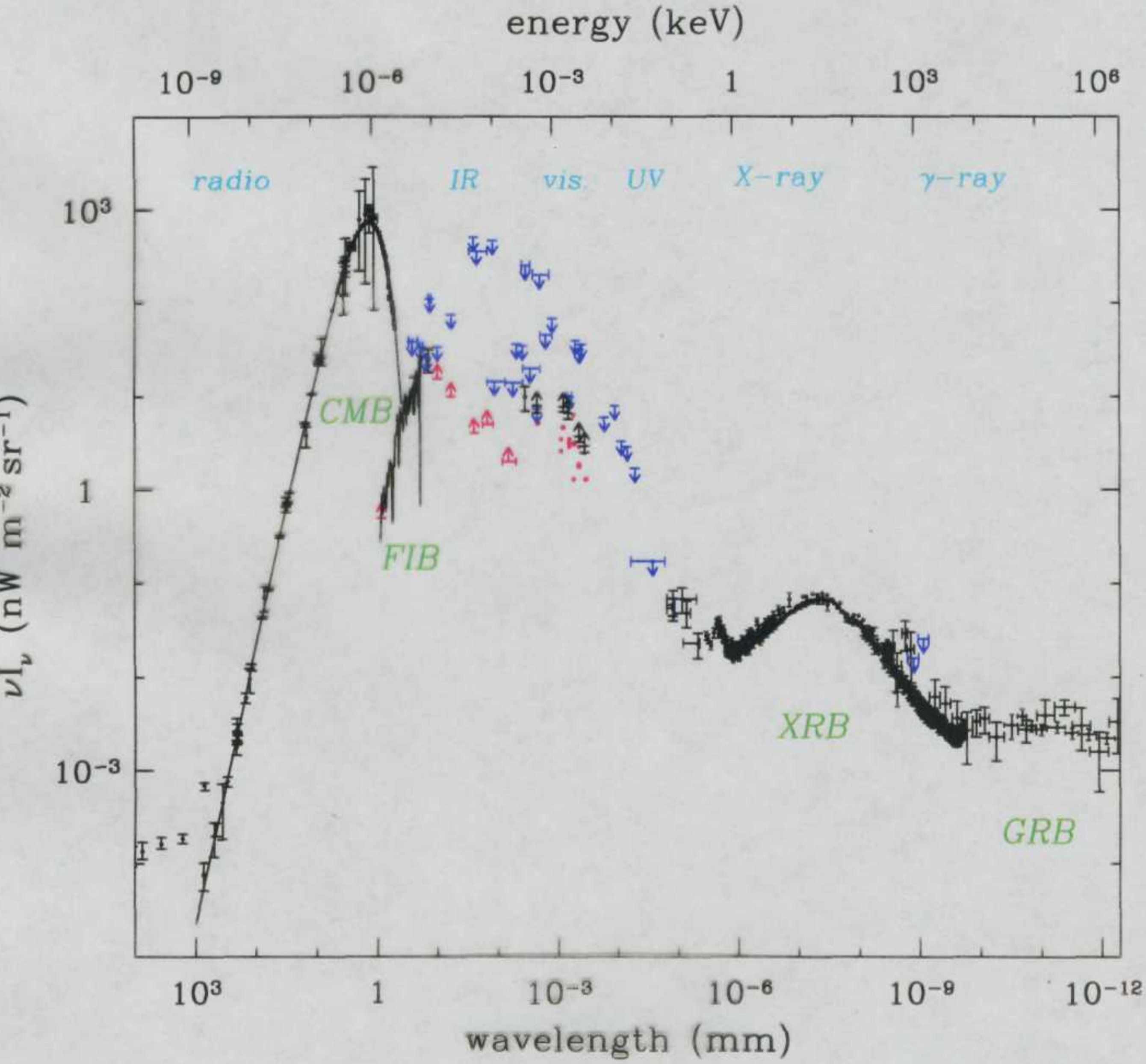
energy (keV)
10^-9
10^-6
10^-3
1
10^3
10^6
radio
IR
vis.
UV
X-ray
γ-ray
10^3
1
10^-3
CMB
FIB
XRB
GRB
νI_ν (nW m^-2 sr^-1)
10^3
1
10^-3
10^-6
10^-9
10^-12
wavelength (mm)

## Поиск анизотропии РИ.

1992 г., COBE спутник $\Theta \simeq 5^\circ \sim \ell \leq 20 \Rightarrow$

открытие неоднородности РИ!

$$\frac{\Delta T}{T} \simeq 20 \text{ мкК}$$

1992 г ÷ 2000: (MAXIMA, DMR, MAX, BAM и др.), баллонные экс

измерение анизотропии РИ при $\ell \lesssim 200$, $\Theta \simeq 1^\circ$.

## MAXIMA-1, BOOMERANG

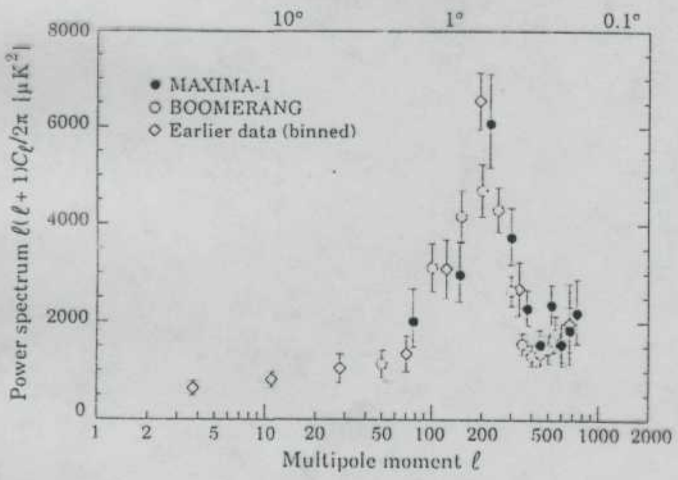


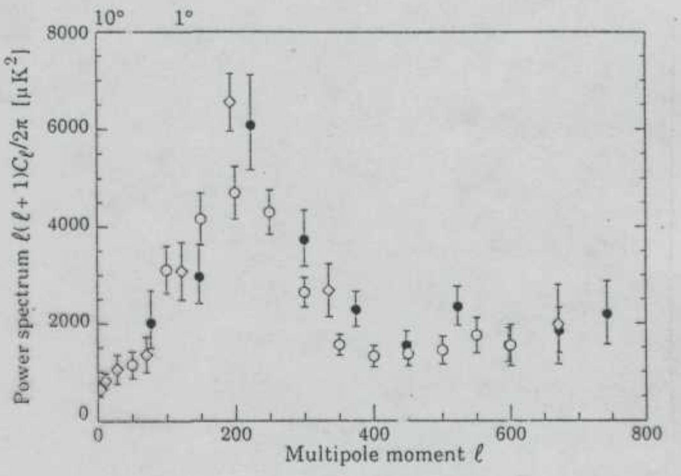


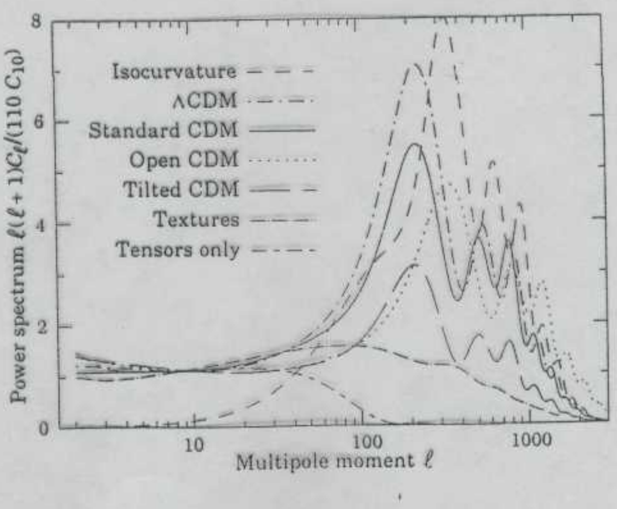

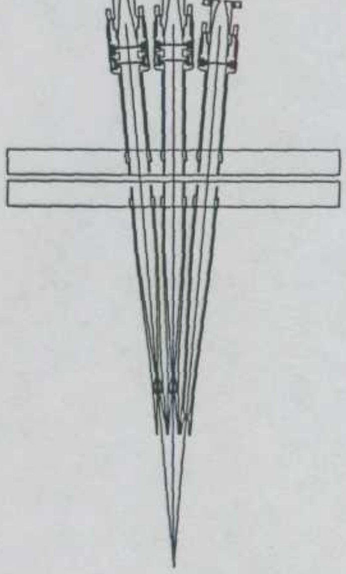

FIGURE 3. Photograph of the interior of the MAXIMA receiver. The focal plane is at the bottom with horns and light pipes extending to the LHe temperature mounting plate. The 100 mK plate which carries the metal-mesh filter holders and bolometer integrating cavities is spaced 0.5 mm above the LHe plate. The $^3He$ refrigerator and heat switch used to conduct the ADR heat of magnetization to $^3He$ refrigerator are visible on the upper right. Each aluminum box (bottom left) contains FET front-end electronics for five channels.

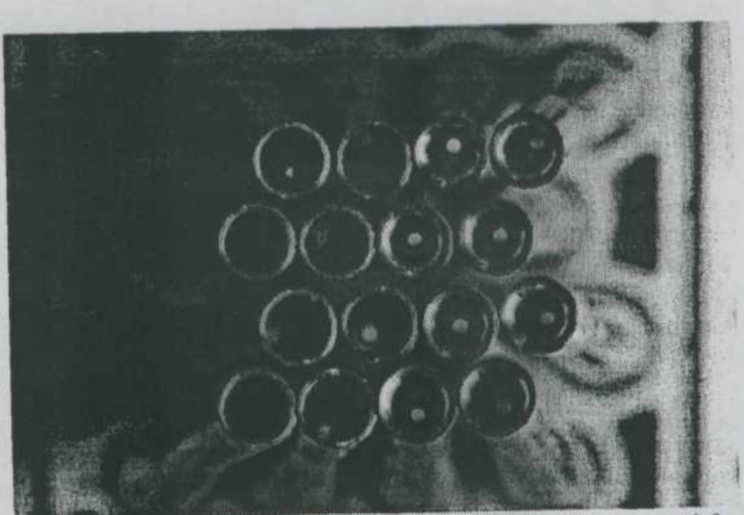

FIGURE 2. Photograph of MAXIMA focal plane. Smooth walled conical horns are used for the eight diffraction-limited 150 GHz channels (two columns to left), and Winston horns are used for the 240 and 410 GHz channels (two columns to right) which detect multiple optical modes. As the array is scanned in azimuth (horizontal in photo), each pixel is measured with four detectors in a row with the three frequency bands. The beamsize for all pixels is 10′. The outer diameter of the horns is ≈ 5.8 mm.

164

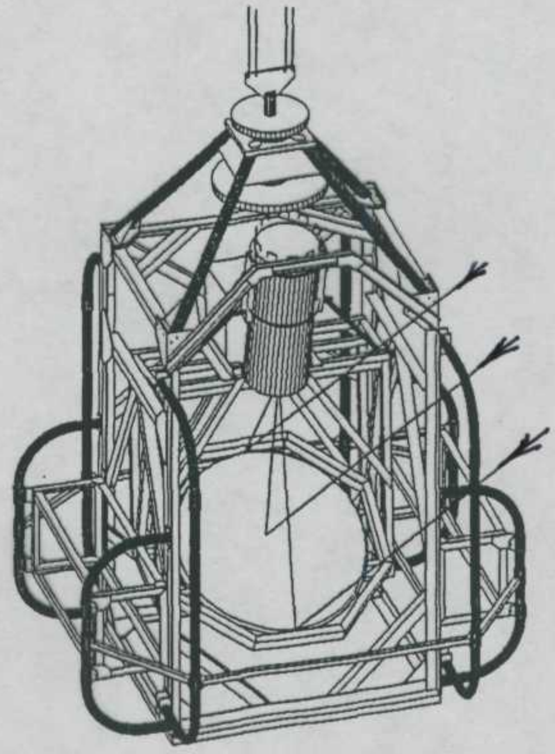

**FIGURE 11.** Drawing of the MAXIMA gondola. The primary mirror and the receiver are mounted to an inner frame supported on trunion bearings to change beam elevation from 20° to 55°. The gondola is largely constructed with bolted aluminum members. The attitude control and data acquisition electronics are housed in the two aluminum boxes on the sides of the gondola.

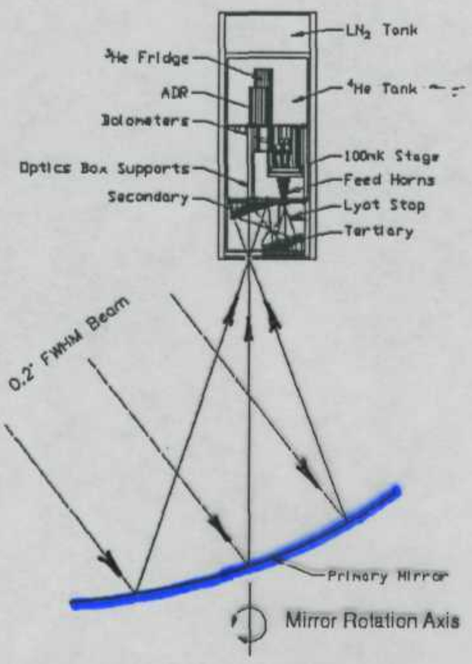


**FIGURE 1.** Cross-section of optical system. The primary mirror is a 1.3 m diameter off-axis paraboloid. The two reimaging mirrors are housed in a well baffled box that is maintained at LHe temperature. The optical system provides a 1° x 1° diffraction-limited field-of-view at 150 GHz. A baffle at the intermediate focus and a Lyot stop provide excellent telescope sidelobe performance. The bolometers are cooled to 100 mK by an Adiabatic Demagnetization Refrigerator. Both LN and LHe cryogen hold times are ≈ 40 hours. The optical entrance to the receiver is vacuum sealed with a window made from 40 $\mu$m thick polypropylene.

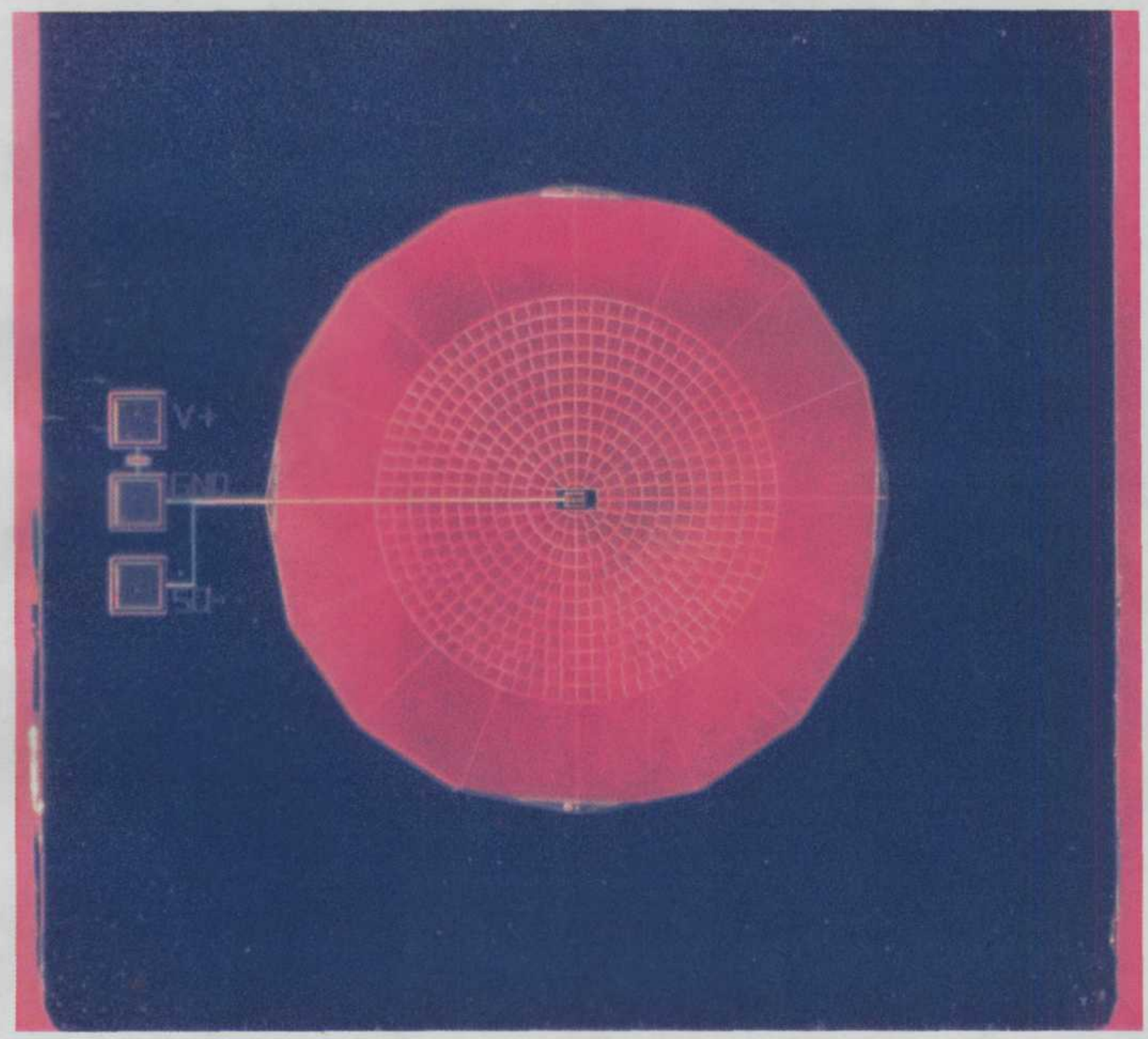


**The micromesh bolometer**, reminicent of a spider's web, uses a free-standing micromachined mesh of silicon nitride to absorb millimeter-wave radiation from the cosmic microwave-background. This design uses the minimum amount of material for optimal performance. Millimeter-wave radiation is absorbed and measured as a minute temperature rise in the mesh by a tiny Germanium thermistor. Cooling the sensor to three tenths of a degree above absolute zero results in the high sensitivity necessary to create the BOOMERANG maps.

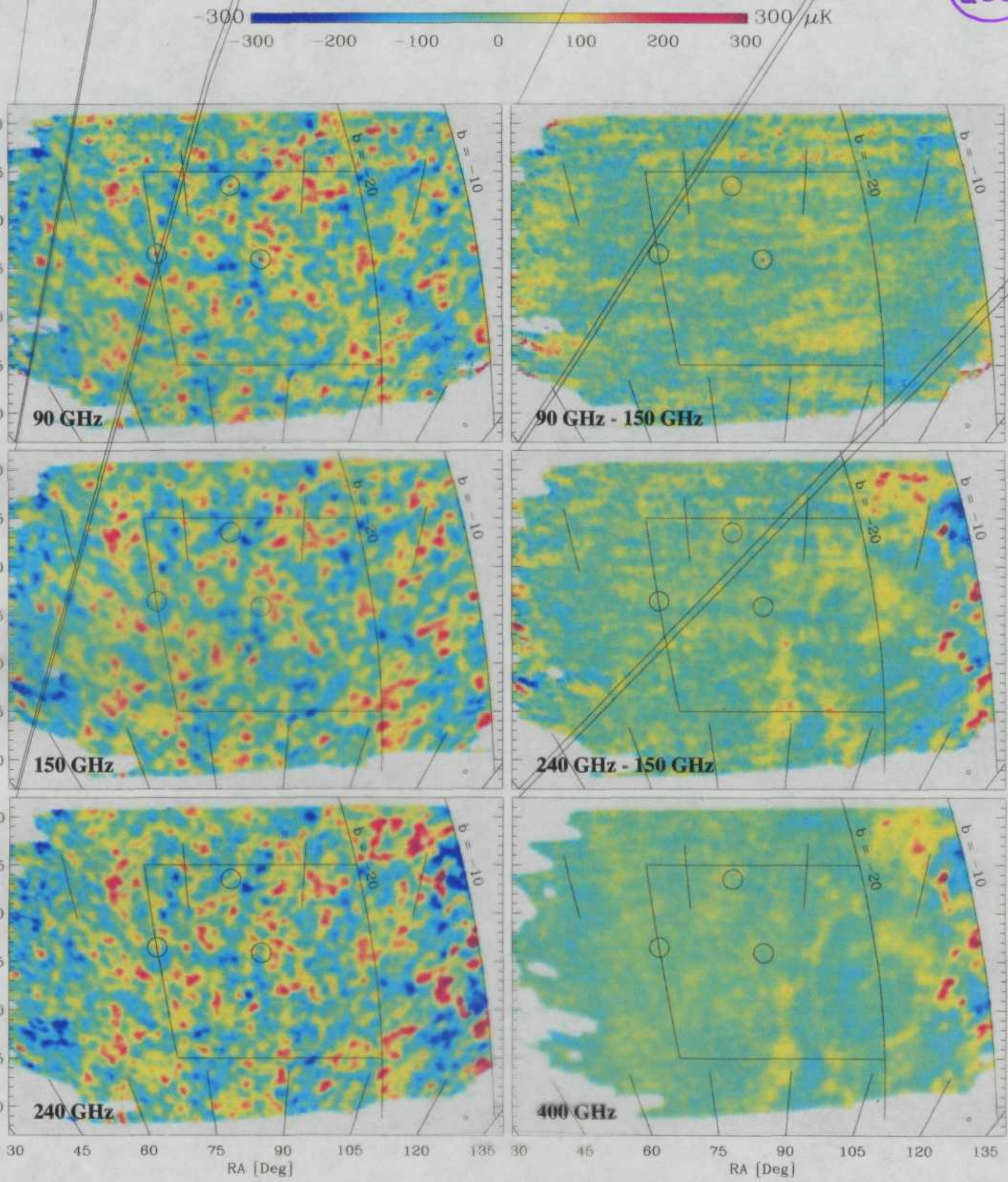
-300
300 μK
-300 -200 -100 0 100 200 300
90 GHz
90 GHz - 150 GHz
150 GHz
240 GHz - 150 GHz
240 GHz
400 GHz
b = -20
b = -10
Dec [Deg]
-30 -35 -40 -45 -50 -55 -60
RA [Deg]
30 45 60 75 90 105 120 135

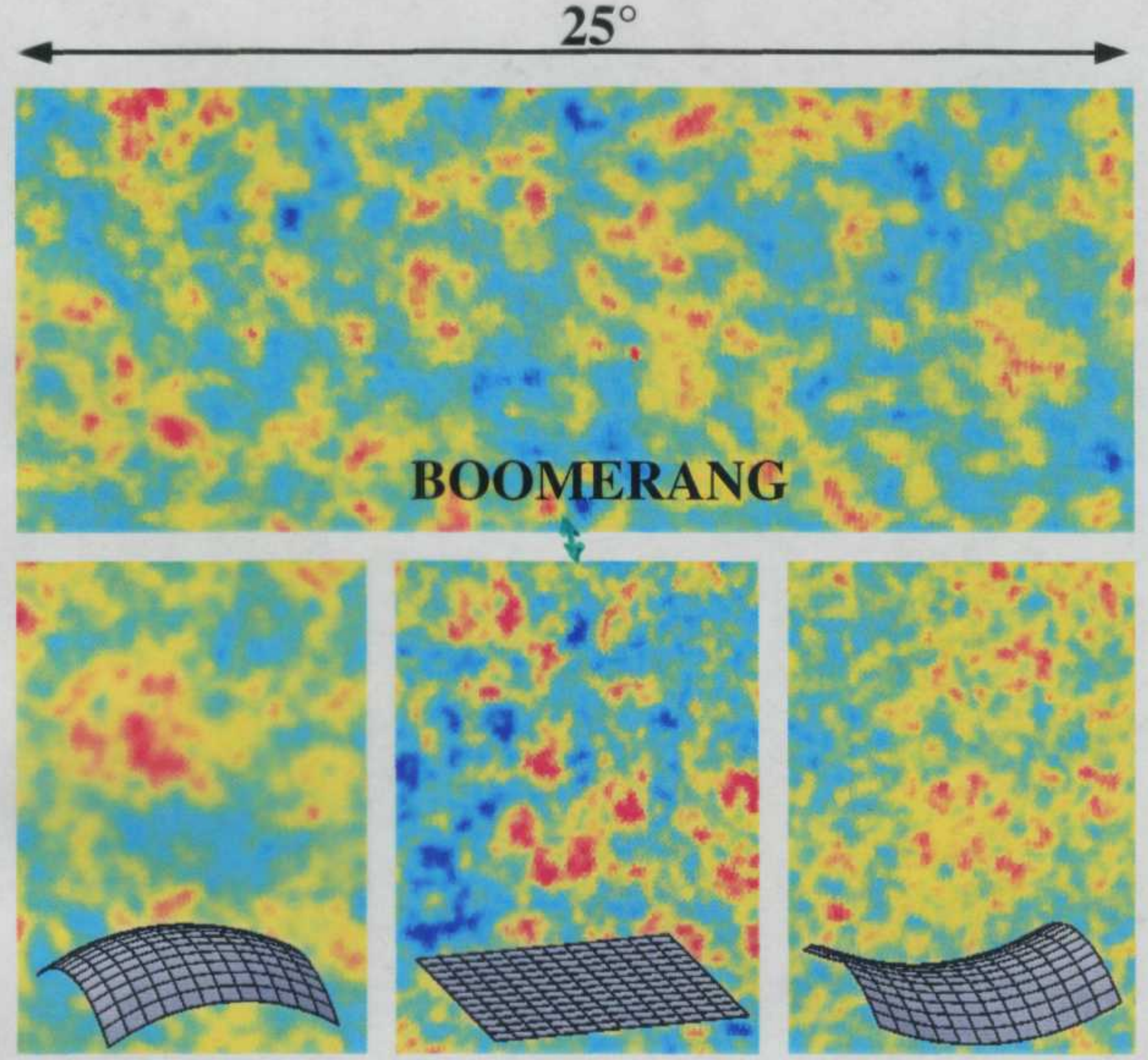


**BOOMERANG images determine the geometry of space.** By observing the characteristic size of hot and cold spots in the BOOMERANG images, the geometry of space can be determined. Cosmological simulations predict that if our universe has a flat geometry, (in which standard high school geometry applies), then the BOOMERANG images will be dominated by hot and cold spots of around 1 degree in size (bottom center). If, on the other hand, the geometry of space is curved, then the bending of light by this curvature of space will distort the images. If the universe is closed, so that parallel lines converge, then the images will be magnified by this curvature, and structures will appear larger than 1 degree on the sky (bottom left). Conversely, if the universe is open, and parallel lines diverge then structures in the images will appear smaller (bottom right). Comparison with the BOOMERANG image (top) indicates that space is very nearly flat.

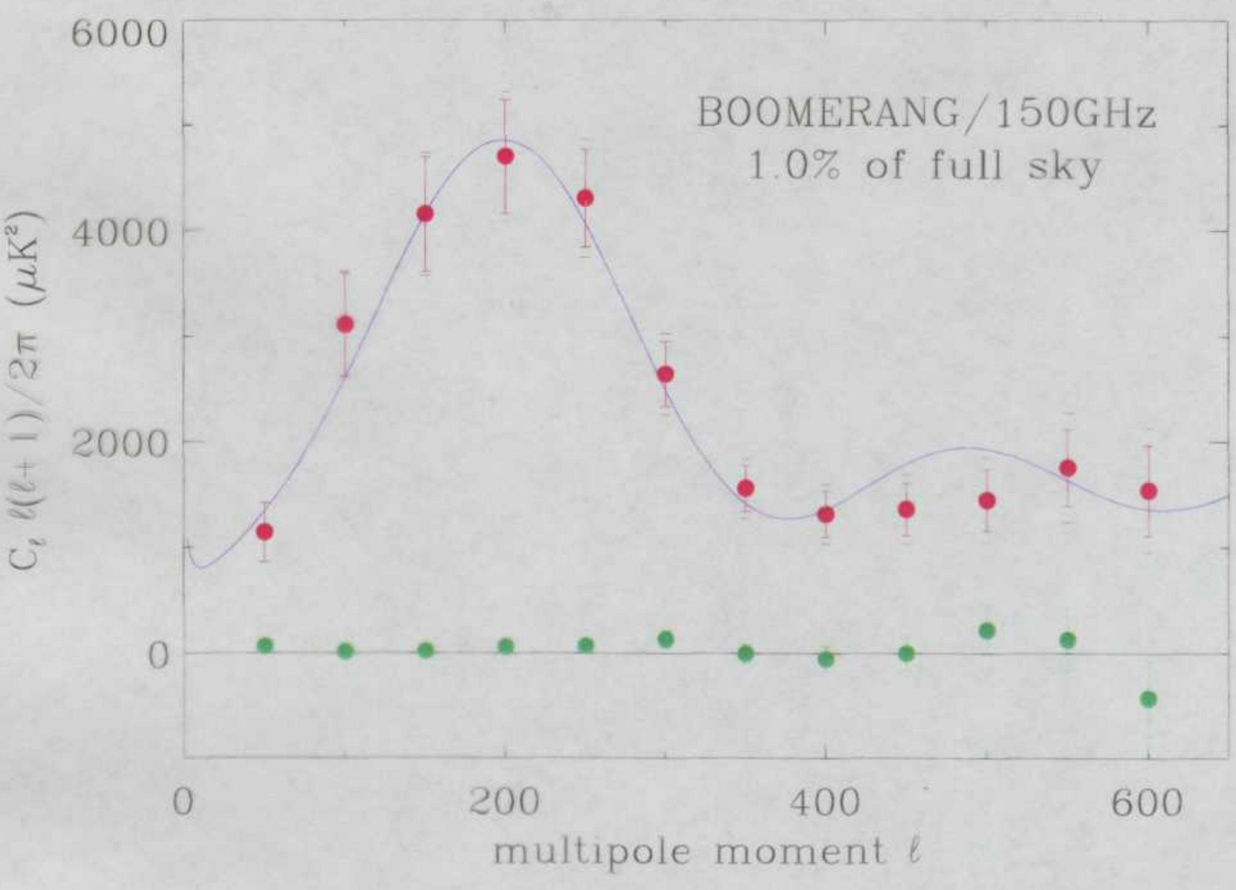

BOOMERANG/150GHz
1.0% of full sky
6000
4000
2000
0
0
200
400
600
multipole moment $\ell$
$C_\ell \, \ell(\ell+1)/2\pi \; (\mu K^2)$

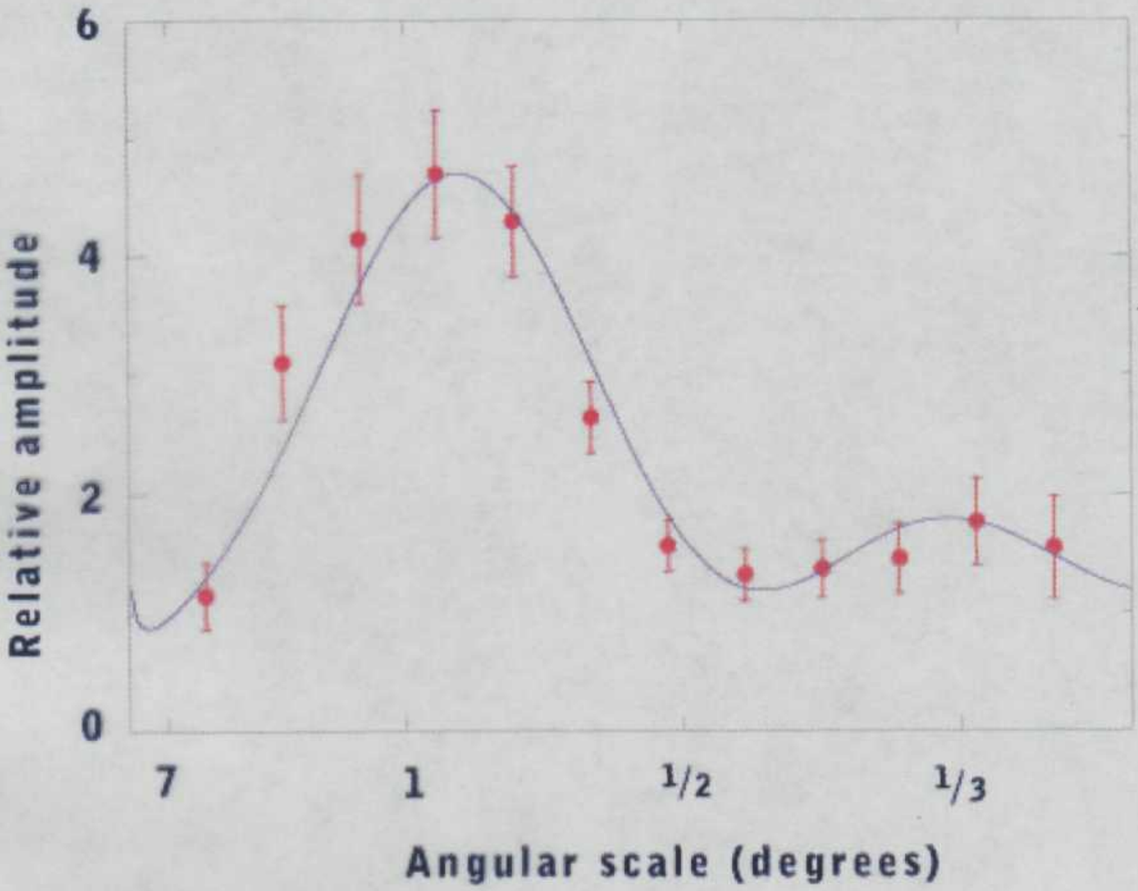


**The Spectrum of Primordial Sound** The temperature variations in early universe seen in the BOOMERANG images are due to sound waves in the primordial plasma. The angular spectrum of these images shown here, reveals the characteristic size of the structures that dominate the image. A peak in this spectrum at scales of ~ 1 degree, as is seen here in the BOOMERANG data, indicates that the Universe is nearly spatially flat. The data can be well fit by cosmological models that contain non-baryonic matter in addition to normal, baryonic matter. One such model is indicated by the solid blue curve. A generic feature of such models is the presence of a harmonic series of additional peaks beyond the fundamental peak at ~ 1 degree. The relative height of the second peak at ~ 1/2 degree on the sky varies with the ballance of matter in the Universe contained in normal or baryonic matter and non-baryonic matter.

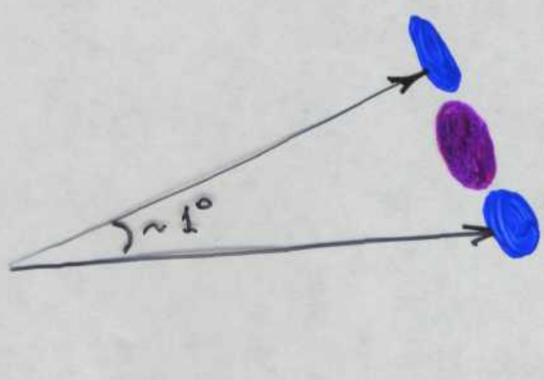

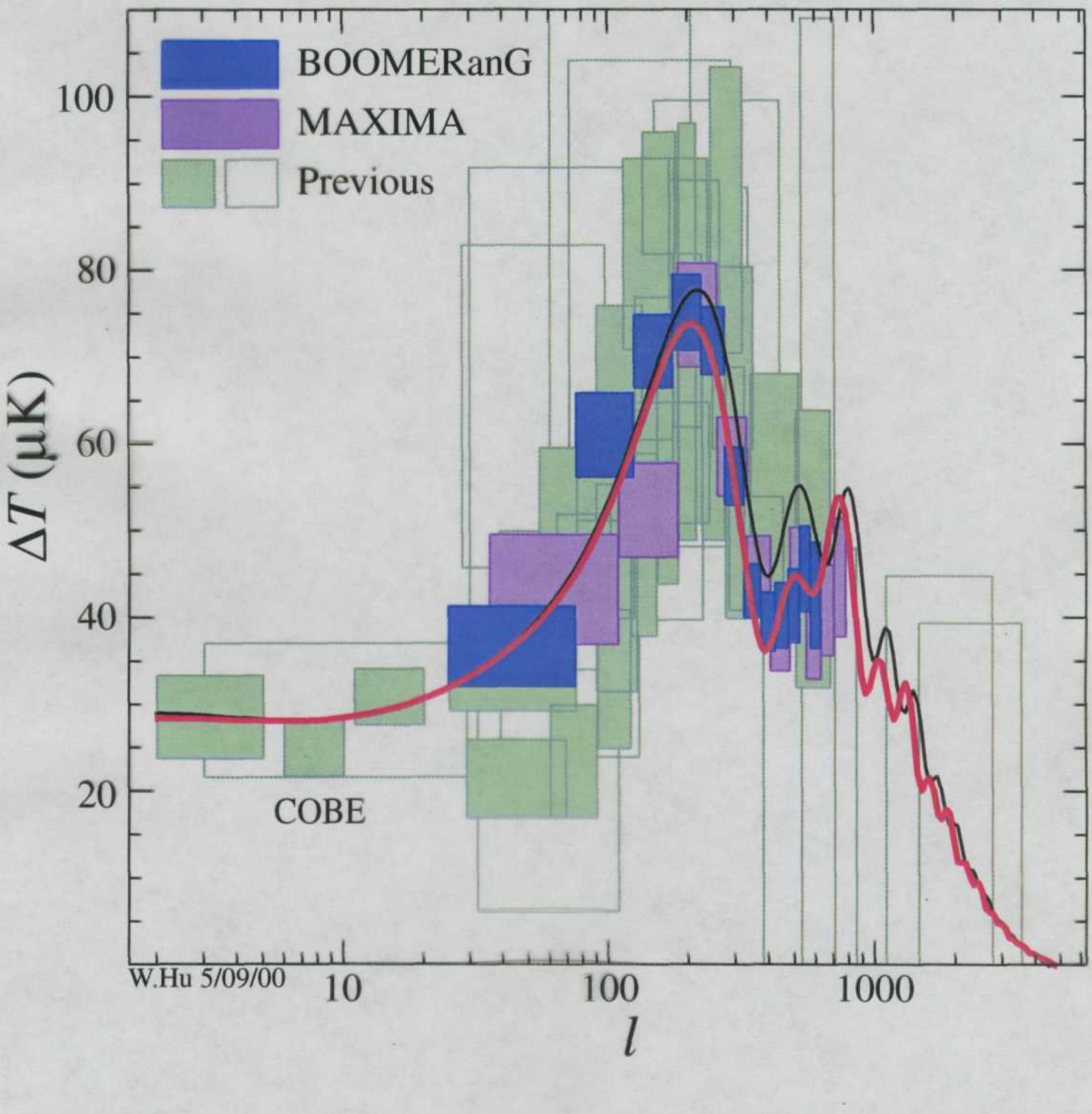

BOOMERanG
MAXIMA
Previous
100
80
60
40
20
ΔT (μK)
COBE
W.Hu 5/09/00
10
100
1000
l

# Основные выводы.

## (MAXIMA-1, BOOMERANG & COBE/DMR)

1. Плоская геометрия Вселенной!

$$\Omega_{tot} = 1.11 \pm 0.07$$

2. Показатель степени спектра начальных флуктуаций плотности

$$n_s = 1.01 \pm^{0.09}_{0.07}$$

(масштабная инвариантность)

3. Барионная плотность:

$$\Omega_b \cdot h^2 = 0.032^{+0.005}_{-0.004}$$

(доминируют другие виды материи.)

4. Согласуются с инфляционной моделью.

5. $\exists^{ие}$ небарионной тёмной материи и антигравитирующего вещества во Вселенной.

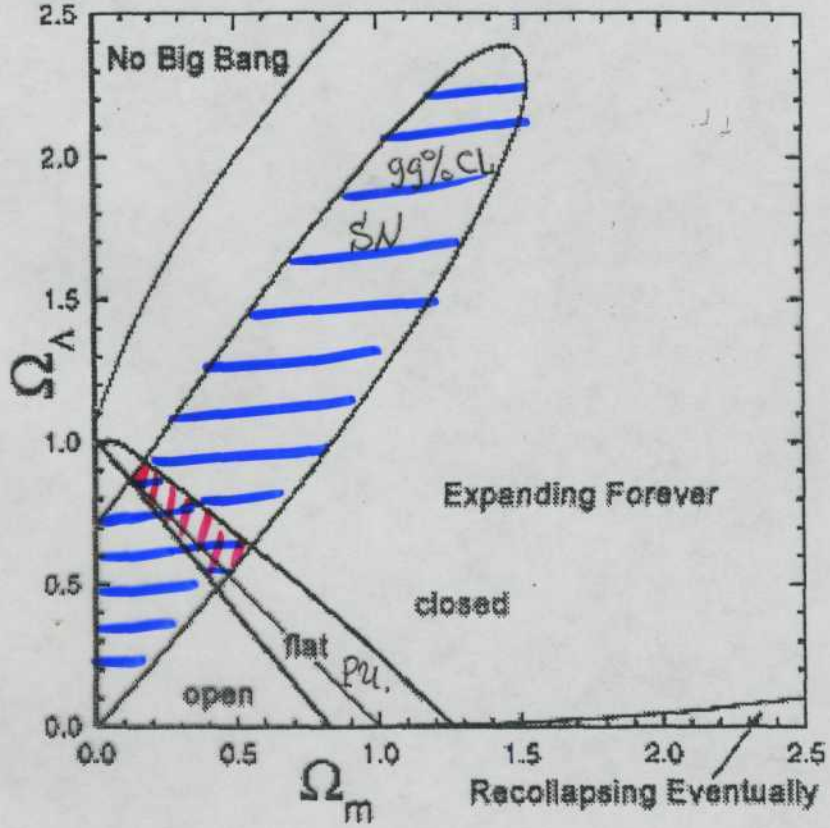


1. Микролинзы $\Omega_m = 0.2 \pm 0.1$

2. SN Ia $-$ $\Omega_m = 0.28 \pm 0.08 \pm 0.05$

в предполож-ии плоской Вселенной.

# Projected Satellite Errors

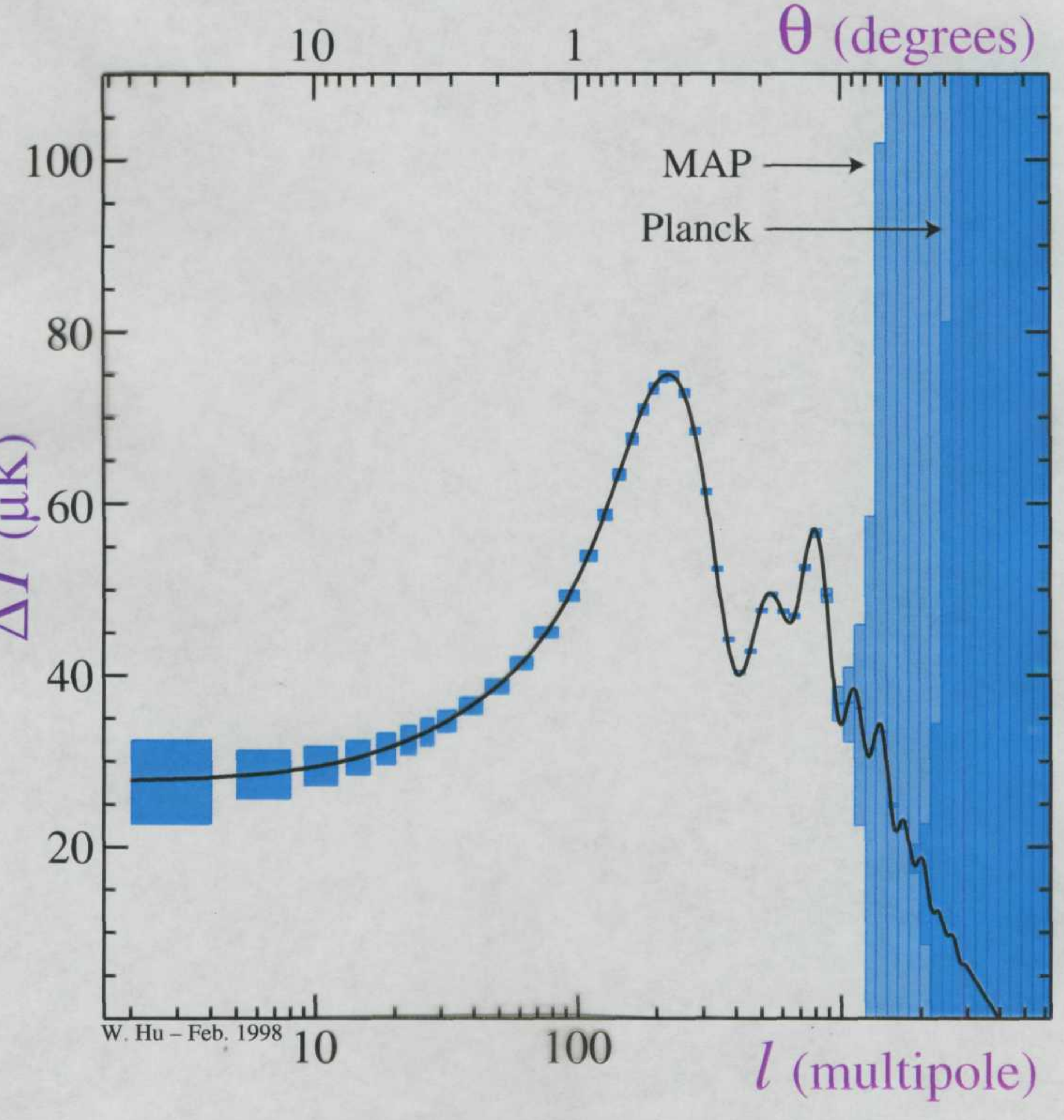

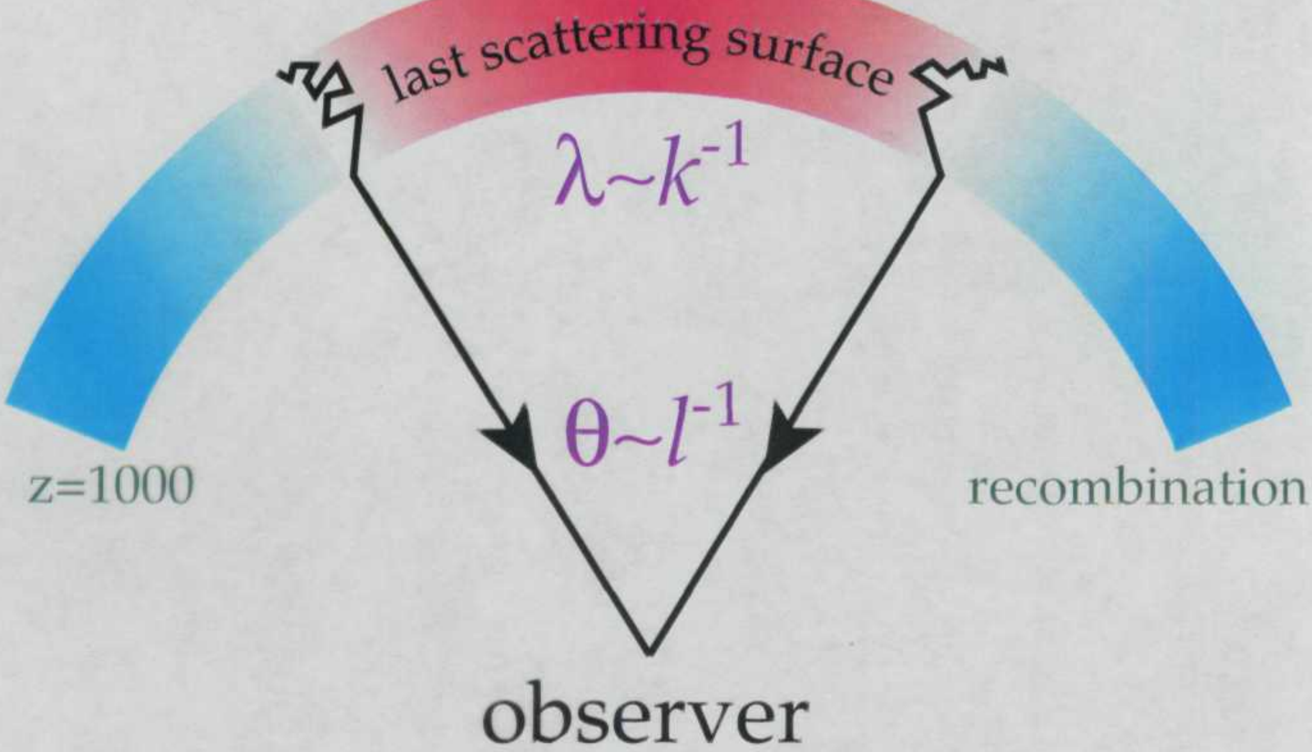
last scattering surface
$\lambda \sim k^{-1}$
$\theta \sim l^{-1}$
z=1000
recombination
observer

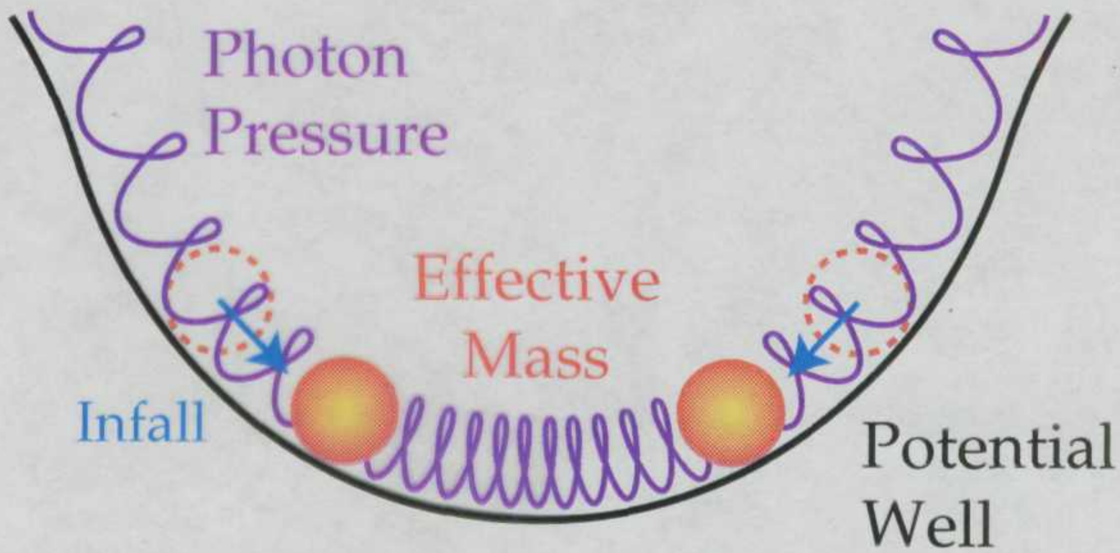
Photon
Pressure
Effective
Mass
Infall
Potential
Well

175

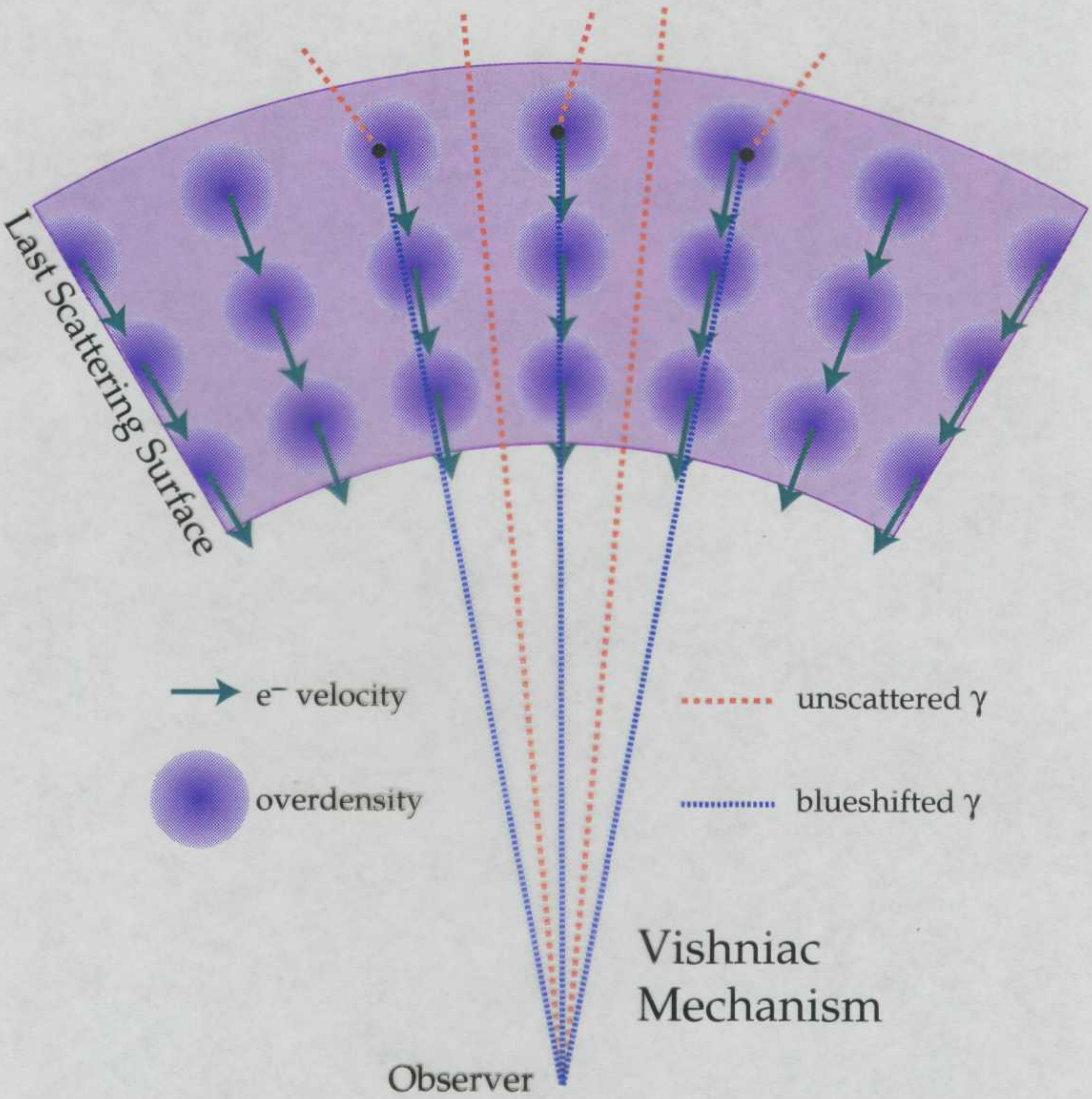


Vishniac
Mechanism